Article:
Botelho MacHado, Carla, Marsh, Robert, Hargreaves, Jessica et al. (2024) Changes in holopelagic Sargassum spp. biomass composition across an unusual year. Proceedings of the National Academy of Sciences of the United States of America. e2312173121. ISSN: 1091-6490

https://doi.org/10.1073/pnas.2312173121

PNAS RESEARCH ARTICLE | ENVIRONMENTAL SCIENCES

Changes in holopelagic *Sargassum* spp. biomass composition across an unusual year

Carla Botelho Machado[a,1], Robert Marsh[b,1], Jessica K. Hargreaves[c], Hazel A. Oxenford[d], Gina-Marie Maddix[e], Dale F. Webber[e], Mona Webber[f], and Thierry Tonon[a,2]

Edited by Nils Stenseth, Universitetet i Oslo, Oslo, Norway; received July 18, 2023; accepted April 6, 2024

The year 2021 marked a decade of holopelagic sargassum (morphotypes *Sargassum natans* I and VIII, and *Sargassum fluitans* III) stranding on the Caribbean and West African coasts. Beaching of millions of tons of sargassum negatively impacts coastal ecosystems, economies, and human health. Additionally, the La Soufrière volcano erupted in St. Vincent in April 2021, at the start of the sargassum season. We investigated potential monthly variations in morphotype abundance and biomass composition of sargassum harvested in Jamaica and assessed the influence of processing methods (shade-drying vs. frozen samples) and of volcanic ash exposure on biochemical and elemental components. *S. fluitans* III was the most abundant morphotype across the year. Limited monthly variations were observed for key brown algal components (phlorotannins, fucoxanthin, and alginate). Shade-drying did not significantly alter the contents of proteins but affected levels of phlorotannins, fucoxanthin, mannitol, and alginate. Simulation of sargassum and volcanic ash drift combined with age statistics suggested that sargassum potentially shared the surface layer with ash for ~50 d, approximately 100 d before stranding in Jamaica. Integrated elemental analysis of volcanic ash, ambient seawater, and sargassum biomass showed that algae harvested from August had accumulated P, Al, Fe, Mn, Zn, and Ni, probably from the ash, and contained less As. This ash fingerprint confirmed the geographical origin and drift timescale of sargassum. Since environmental conditions and processing methods influence biomass composition, efforts should continue to improve understanding, forecasting, monitoring, and valorizing sargassum, particularly as strandings of sargassum show no sign of abating.

algal blooms | biochemical composition | elemental composition | processing | volcanic ash

Over the last two decades, there has been an increasing number of reports describing seaweed (macroalgae) invasions and blooms affecting coastal environments and populations worldwide (1). These seaweed events have become more frequent and impactful as the Anthropocene unfolds, with no sign of abating. They have a wide impact on coastal biodiversity and communities and can exacerbate important socioeconomic and health problems (2). One example of recent and now recurrent seaweed bloom events is the Great Atlantic Sargassum Belt (GASB) (3), caused by floating mats of holopelagic sargassum species (brown algae). Since 2011, annual stranding of millions of tons of sargassum biomass has become a new normal in the Caribbean and West Africa (4). Several hypotheses have been suggested to explain the emergence and recurrence of these sargassum events, including physical (5) and chemical (6) drivers associated with climate change and variability across the Tropical Atlantic (7).

This holopelagic sargassum (referred to as sargassum hereinafter) biomass is formed by assemblage of the morphotypes *Sargassum natans* I, *S. natans* VIII, and *Sargassum fluitans* III (8, 9). It represents an important element in carbon cycling and sequestration at the local scale (10). In the initial years of sargassum events, the stranded biomass was seen as a waste and most of it was discarded in landfills. However, in recent years, several directions have been explored for its valorization (11), including the production of bioenergy as liquid fuels (12, 13) and biogas (14–16), bioremediation (17), and for soil amelioration (18, 19). Sargassum events are still considered an emergent risk (20), and progress has been made regarding governance and management policies (21). One of the important parameters to consider for the implementation of valorization through industrial processes is potential changes in biomass composition depending on processing methods, as feedstock needs to be stabilized before subsequent uses. In line with this, we have previously explored the impact of sample processing (frozen vs. sun-dried sargassum) using biomass harvested during the summer 2020 in Jamaica (22). This study showed that this aspect of the valorization chain had a significant impact on some of the key biochemical compounds of the sargassum biomass that are also important for the support of its commercial applications, including alginate, fucoxanthin, and phenolics. Another potential issue is

Significance

Since 2011, Caribbean and West African countries have been affected by millions of tons of stranding sargassum, impacting coastal ecosystems, economies, and human health. Sargassum biomass harvested in Jamaica throughout 2021 shows seasonal changes in morphotype abundance and limited variation in biochemical composition. For valorization, shade-drying vs. freeze-drying decreased phlorotannin, fucoxanthin, and alginate contents, but not total proteins. The year 2021 was also marked by the La Soufrière volcanic eruption in the Caribbean. We suggest that floating sargassum and volcanic ash shared the sea surface for ~50 d, approximately 100 d before reaching Jamaica, and this impacted the elemental composition of stranded biomass. This observation gives new insights into assimilation of elements by sargassum under different influences, like volcanic ash.

Author contributions: R.M., M.W., and T.T. designed research; C.B.M., R.M., G.-M.M., D.F.W., and M.W. performed research; H.A.O. contributed new reagents/analytic tools; C.B.M., R.M., J.K.H., H.A.O., G.-M.M., D.F.W., M.W., and T.T. analyzed data; and C.B.M., R.M., J.K.H., H.A.O., G.-M.M., D.F.W., M.W., and T.T. wrote the paper.

The authors declare no competing interest.

This article is a PNAS Direct Submission.

[1]C.B.M. and R.M. contributed equally to this work.

[2]To whom correspondence may be addressed. Email: thierry.tonon@york.ac.uk.

This article contains supporting information online at https://www.pnas.org/lookup/suppl/doi:10.1073/pnas.2312173121/-/DCSupplemental.

Published May 28, 2024.

the consistency of the feedstock and potential seasonal variations (23). Stable value chains require predictable inputs of biomass combined with a high content of the desired constituents, e.g., alginates that can be used as thickening agents in different industries, or bioactive compounds (e.g. fucoxanthin) that can be used in functional food (nutraceuticals) or in cosmetics. The EU-Roadmap for the blue economy reported that the seasonal variation in biomass composition is a characteristic of seaweeds that can affect the scalability of production and the logistical processes (24). In the last few years, there have been increasing reports on seasonal variations of the biochemical (25–27) and elemental (28–30) composition of sargassum, as well as on seasonal changes in the morphotype abundance (31–35).

Our focus here is on the 2021 sargassum season, during which a substantial bloom was evident across the Equatorial Atlantic from spring. This bloom was potentially exposed to the major eruption of La Soufrière volcano, located on the island of St Vincent, which persisted for around ten days from 9th of April 2021. The eruption produced an extensive plume at high altitude that dispersed and deposited ash eastward, as predicted in previous atmospheric simulations (36) and subsequently observed through April 2021 (37). Considering the transport pathways of sargassum, the ash deposition pattern had the potential to impact Caribbean-bound sargassum. Volcanic ash fertilization of the surface ocean has previously been observed in situ in the iron-limited extratropics in the northeast Pacific following eruption of the Kasatochi volcano in the Aleutian island-arc in August 2008 (38), and in the subpolar North Atlantic after the spring 2010 Eyjafjallajökull volcanic eruption in Iceland (39). These natural fertilization events were associated with massive and temporary increase of phytoplankton biomass. However, no study has as yet investigated the potential impact of volcanic ash on the biochemical and elemental composition of floating seaweeds.

In this context, the current study had three main objectives: i) to investigate potential seasonal changes in the morphotype abundance as well as in the biochemical and elemental composition of beached sargassum; ii) to assess how the processing of seaweed may affect the consistency of the feedstock; iii) to determine whether sargassum mats have been in contact with volcanic ash and how this may have influenced their biochemical and elemental composition.

Results

Satellite Observations at the Regional Scale. Areas of sargassum over the annual cycle were aggregated for eight selected subregions by sampling FA_density data (Fig. 1). The three subregions of the Central Atlantic (Fig. 1 *A*–*C*) follow previous analysis (5) and were motivated by broad separation of dynamical regimes. The East Caribbean region is split into East, Central, and West subregions (Fig. 1 *D*–*F*). The north and south of Jamaica (Fig. 1 *G* and *H*) were separately considered following a previous forecasting approach (40). Data for 2021 are plotted with the thick lines, alongside corresponding data for 2011 to 2020 (thin lines), to indicate when and where sargassum in 2021 was exceptionally extensive. We additionally indicate (with green shading) the 10-d duration of the La Soufrière eruption (9 to 18 April).

We remark here on some general features of the 2021 area coverage, relative to the previous years of extensive sargassum. First, we note that the period of eruption coincided with a substantial reduction in sargassum area detected in the Western Tropical North Atlantic (Fig. 1*C*). This was likely a consequence of reduced visibility, consistent with the widespread extent of ash particles in the atmosphere to the east of La Soufrière volcano. Following this period of reduced visibility, areas of sargassum substantially increased in the upstream Central Equatorial North Atlantic (Fig. 1*A*), to an extent that exceeds all previous years over days 115 to 125 (late April to early May). Sargassum area in the Western Tropical North Atlantic likewise increased at this time to a level exceeded only in 2018, leading to record mid-summer 2021 peaks through days 150 to 155 (early June) and days 175 to 205 (late June to late July).

Turning attention to the Caribbean, we note that sargassum area remained exceptionally high late into the summer of 2021, reaching and sustaining record levels over days 215 to 275 (August to September) in the East sector (Fig. 1*D*), most notably over days 240 to 275 (September) in the Central sector (Fig. 1*E*), and to a lesser extent in the western sector (Fig. 1*F*). Of consequence for beaching around Jamaica (Fig. 1 *G* and *H*), areas of sargassum were relatively high through late summer, more remarkably for the southern sector, where areas exceeded previous records over days 250 to 270 (most of September). Noting the progressively later timing of excessive sargassum areas, and moving from the Central Atlantic, across the Caribbean, to the Jamaican region, we have considered below the associated advective timescale for drifting sargassum, based on simulated forward trajectories from the vicinity of volcanic ash deposition and backward trajectories from the vicinity of Jamaica.

Simulating Drift of Sargassum and Volcanic Ash. To examine the possible influence of volcanic ash on sargassum across the Caribbean region during spring and summer of 2021, their potential common drift timescales and pathways were evaluated. By comparing the likely trajectories of ash and sargassum, we assessed the extent to which specific elements associated with the volcanic ash would have been available to the floating biomass, hence potentially influencing the biochemical and elemental composition of the floating seaweeds. Of importance was the likely difference between the timescales and pathways due to ash moving with the seawater, while exposed sargassum moves also in response to surface winds; this should lead to a natural and progressive downstream divergence of ash and sargassum.

We first considered ash deposition over an idealized triangular area, based on observed dispersal of the plume (37), extending from St. Vincent eastward to 50°W at 14°N and progressively southward to 6°N (at 50°W). We seeded this area with particles in constant concentration, added over 5 d. From this triangular area, we forward-tracked both "sargassum particles," based on an initial distribution in early April 2021, subject to 1% windage, and "ash particles," identically distributed but drifting with surface currents only. All particles were tracked for 180 d, sampling currents and winds for a representative model hindcast year (1988). In Fig. 2, we showed the fractional coverage and age statistics for the "sargassum" and "ash" particles. There was a notable divergence of pathways, with advection of sargassum particles that is more westward (Fig. 2*C*) compared to the north–westward advection of ash particles (Fig. 2*A*). Combined with the age statistics (Fig. 2 *B* and *D*), we evaluated a timescale of ~50 d over which sargassum "shared" the surface layer with ash, assuming this to remain present on the same timescale.

To further evaluate the provenance of sargassum reaching Jamaica in late summer, we backtracked particles from this location and time, obtaining the statistics shown in Fig. 3. The distribution of fractional presence in Fig. 3*A* clearly reveals a primary pathway via the western boundary current system, from the equatorial Atlantic and through the Caribbean. The drift timescale from Barbados to Jamaica was around 100 d, considering the upstream flow located south of Barbados (Fig. 3*B*). This pathway and timescale could be further related to the potential upstream

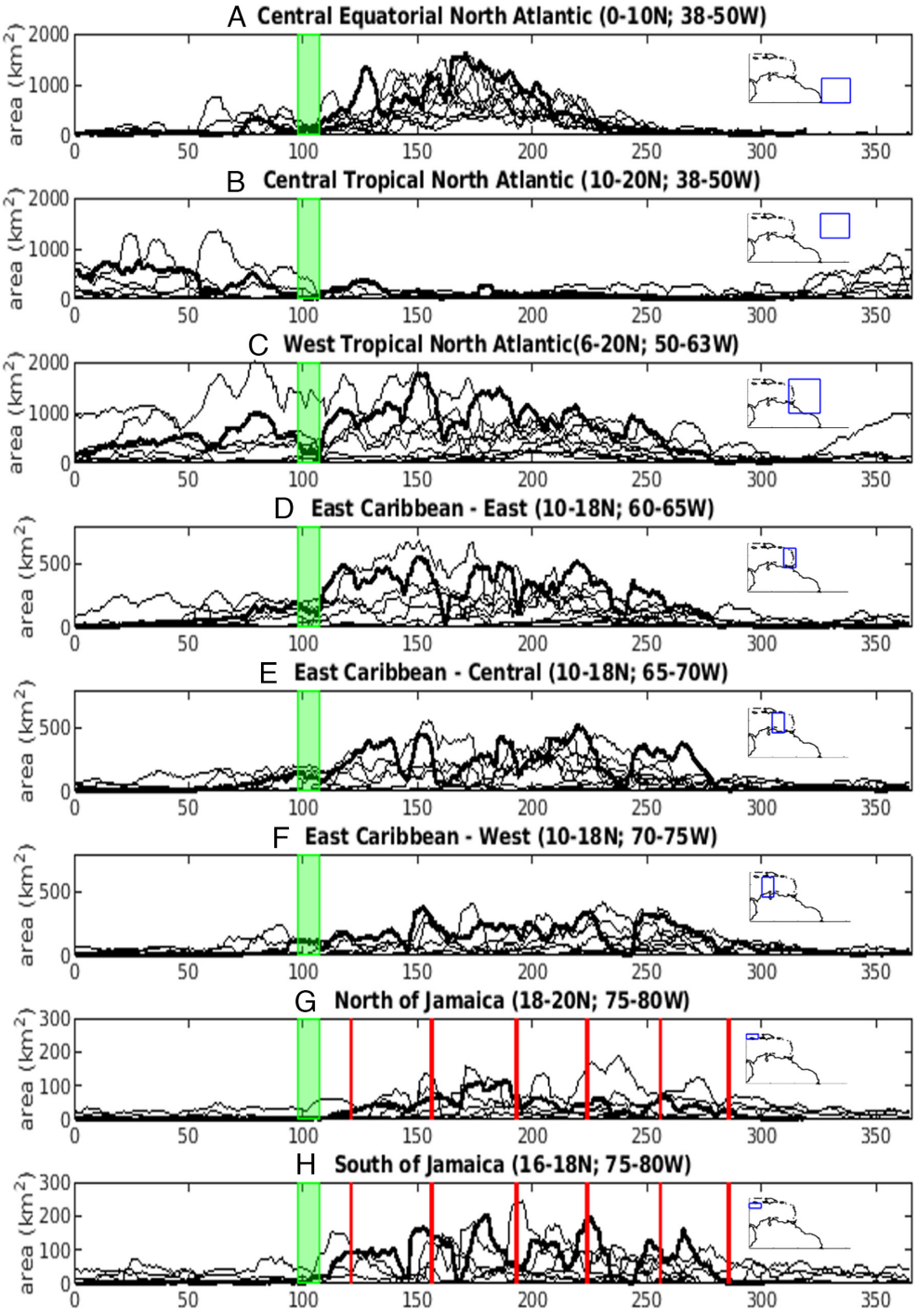

Fig. 1. Regionally aggregated areas (km^2) of sargassum: (*A*) Central Equatorial North Atlantic; (*B*) Central Tropical North Atlantic; (*C*) West Tropical North Atlantic; (*D*) East Caribbean–East; (*E*) East Caribbean–Central; (*F*) East Caribbean–West; (*G*) North of Jamaica; (*H*) South of Jamaica. Thick curves indicate 2021, thin curves indicate 2011 to 2020, and green shading indicates the timing and duration of the major La Soufrière eruption (9 to 18 April). In *G* and *H*, red vertical lines indicate the timing of beach sampling over May–October in the south of Jamaica.

influence of ash fallout from La Soufrière volcano, as the particles were backtracked from August. Considering the broad region from the Lesser Antilles to the equatorial zone, mean age in the range of 90 to 120 d indicated that particles arriving off east Jamaica in early August transited this region between early April and early May. Given the eastward dispersion and deposition of ash across the same region, we suggest that the sargassum arriving east of Jamaica in early August was likely exposed to ash fallout.

We further noted high fractional presence to the north of Jamaica, with age (days prior to arrival) increasing to the west, indicating that some of the particles (hence sargassum) arriving off east Jamaica may have arrived via a longer and hence slower clockwise round-island flow. These particles drift westward to the south of Jamaica, almost reaching the Yucatan Channel before returning to the east. This alternative pathway provided additional context for drift timescale, and the extent to which sargassum may have been subject to ash fallout, if located east of the Lesser Antilles prior to the eruption of La Soufrière.

Changes in Morphotype Abundance within Sargassum Biomass Harvested in Jamaica. Sargassum mats present in the Equatorial Tropical Atlantic Ocean are formed by the aggregation of two different species represented by three distinct morphotypes: *S. natans* I, *S. natans* VIII, and *S. fluitans* III. So far, no investigation of potential variations of abundance of these morphotypes across a full year of inundations events in Jamaica has been conducted. Our data showed clear and significant changes in the abundance of the three identified morphotypes throughout the year 2021 (Fig. 4 and Dataset S1 A–C). *S. fluitans* III was the most abundant species in all samples analyzed, with values ranging between 59 and 86%

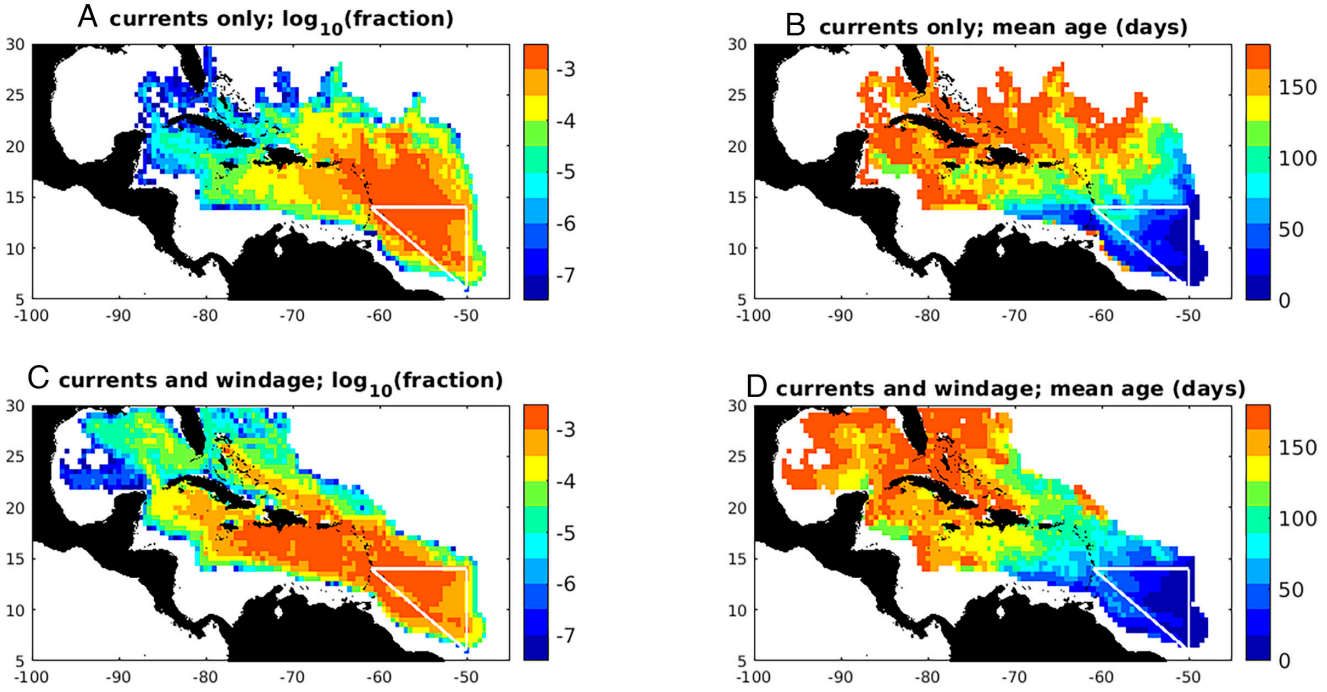

Fig. 2. Statistics of simulated 180-d forward trajectories from the triangular area representative of volcanic ash deposition in early April: (*A*) fractional presence and (*B*) mean age, drifting with surface currents only (simulating ash dispersal); (*C*) fractional presence and (*D*) mean age, drifting with surface currents and subject to 1% windage (simulating sargassum dispersal).

of the biomass DW. Quantities of *S. natans* fluctuated significantly with *S. natans* I being the most abundant of the two morphotypes all year round (13 to 32% of biomass DW). *S. natans* VIII was less abundant at the end of the 2021 season, with up to 10% biomass DW in September and October. Profiles were very similar between May and October, June and September, and July and August.

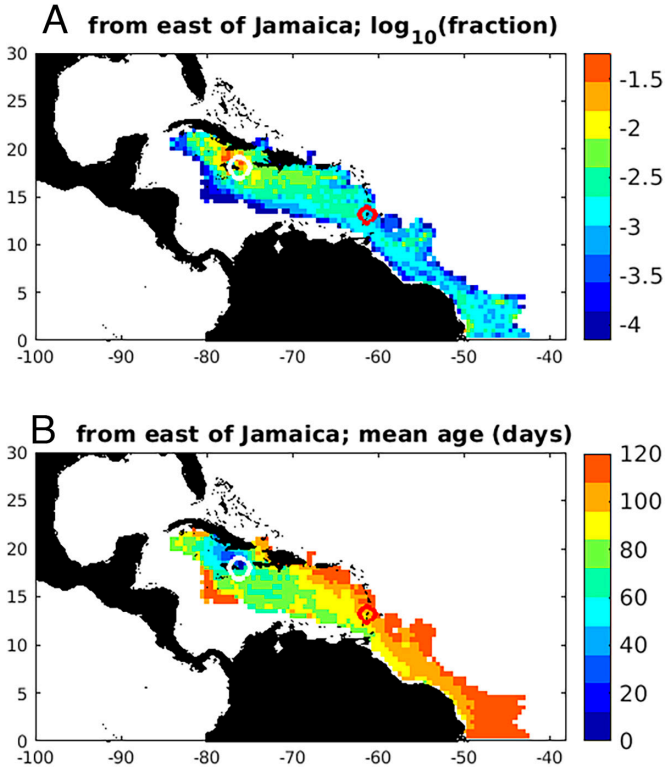

Fig. 3. Statistics of simulated 120-d backward trajectories for August released over 1988 to 2010 off east Jamaica (white circle): (*A*) fractional presence; (*B*) mean age (days before arrival off Jamaica). St Vincent is indicated with a red circle.

Elemental Composition of La Soufrière Volcanic Ash and Potential Influence of Ash Exposure on Floating Sargassum. Composition of two samples of ash that had fallen on Barbados on the 11th and 13th April 2021 during the main deposition event of the La Soufrière volcanic eruption was analyzed. Elemental content in both samples was very similar, with Al, Ca, Fe, Na, and Mg being the most abundant elements with amounts above 15,000 ppm (Table 1).

While macroalgae elsewhere in the tropics have been demonstrated to be iron-limited (41), it is long established that *S. natans* and *S. fluitans* in the western North Atlantic are phosphorus-limited (42), with iron-limitation not examined. The cumulative deposition of volcanic ash during April may have raised the local concentrations of iron and phosphorus substantially above background levels, and these elements could have been assimilated by floating sargassum. To test this hypothesis, we considered background elemental concentrations in seawater across the region of interest and available from the eGEOTRACES Electronic Atlas (https://www.geotraces.org/geotraces-intermediate-data-product-2021/) for the Western Atlantic GA02 section (43). Taking phosphate as an example, we noted from climatology that dissolved inorganic phosphate in the upper ocean was well below 0.5 μmol kg^{-1} seawater in the region during April (44). This corresponded to a background concentration of 0.5 μmol kg^{-1} seawater of phosphorus. We then proceeded to estimate the implied concentration of phosphorus associated with ash in seawater.

Taking a representative deposition depth of 1 cm of ash across a broad area with a deposit density of 1,200 kg m^{-3} (36), and a mean (averaging BM1 and BM2) phosphorus content of 515 ppm (Table 2), we obtained an integral phosphorus flux (over the deposition timescale) of 0.01 × 1,200 × 515/10^6 = 0.00618 kg m^{-2}. Assuming rapid mixing throughout an April surface mixed layer in this region with representative thickness 50 m (45), this corresponds

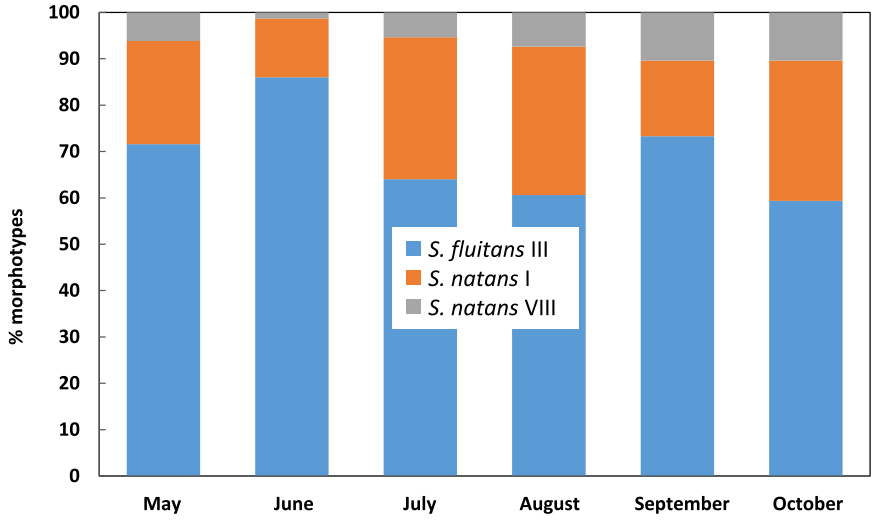

Fig. 4. Relative abundance of the three sargassum morphotypes across the 2021 season in Jamaica. Results of statistical analysis, including of the post hoc test, are provided in Dataset S1 A–C.

to a seawater phosphorus concentration of 1.236×10^{-4} kg m^{-3}, or 0.1236 g m^{-3}. Taking the molar mass of phosphorus (1 mol = 30.97 g), we obtain a concentration of 0.00399 mol m^{-3}; taking seawater density 1,023 kg m^{-3}, this amounts to 3.90×10^{-6} mol kg^{-1} of phosphorus in seawater, or 3.90 µmol kg^{-1} for direct comparison with climatology (maximum 0.5 µmol kg^{-1}). A minimum enrichment factor was thus estimated at 7.8. We concluded that the cumulative deposition of volcanic ash during April may have raised the local concentration of phosphorus in the upper ocean by (at least) almost an order of magnitude above background levels. Repeating this for the other trace elements measured in ash and available from the eGEOTRACES atlas, we summarize the estimated mixed layer concentrations for Al, Fe, Mn, P, Zn, Co, and Ni in Table 2. On the basis of these estimates, it appears that the highest potential seawater enrichment was in Fe and Al, for which concentrations increased over background levels by four to five orders of magnitude; Mn and Co were enriched by three to four orders of magnitude, followed by Zn and Ni. Whether such enrichment levels are consequential for sargassum depends on both the utility and bioavailability of these elements. To the extent that the elements are assimilated into growing sargassum and biologically inert, they can provide information on an upstream encounter with the ash fallout, and thus inform on the geographical origin and drift timescale of floating sargassum, as considered in the next section.

Table 1. Elemental composition of ash collected in Barbados on the 11th (BM1) and the 13th (BM2) of April 2021, Only shown are elements with content >10 ppm and As. The mean ± SD is reported for each measurement

Elements	BM1	BM2
Al	88,359.87 ± 599.84	86,944.36 ± 1,436.78
Ca	62,171.10 ± 329.44	61,261.41 ± 509.27
Fe	51,005.63 ± 1,884.46	48,450.25 ± 784.88
Na	24,050.41 ± 245.12	24,770.91 ± 178.63
Mg	20,435.85 ± 518.77	17,673.39 ± 350.84
Ti	4,848.69 ± 169.45	4,824.63 ± 49.00
K	3,722.97 ± 97.436	3,963.50 ± 40.11
Mn	1,152.47 ± 20.79	1,106.06 ± 8.36
P	495.80 ± 12.13	533.75 ± 3.30
Sr	216.56 ± 1.09	220.65 ± 3.16
V	195.36 ± 15.10	177.61 ± 4.43
Ba	104.68 ± 2.22	112.59 ± 1.44
Cu	83.75± 0.70	93.60 ± 6.12
Zn	81.48 ± 2.10	76.06 ± 0.85
Zr	73.68 ± 2.60	78.45 ± 0.83
Cr	34.25 ± 5.82	28.78 ± 0.84
Sc	26.65 ± 0.59	24.78± 0.04
Y	22.96 ± 0.44	24.25 ± 0.25
Co	17.79 ± 0.74	16.11 ± 0.18
Ni	14.66 ± 0.836	12.32 ± 0.27
Ce	12.35 ± 0.28	13.27 ± 0.12
Rb	9.99 ± 0.30	10.77 ± 0.13
As	1.23 ± 0.04	1.35 ± 0.03

Elemental Composition of Stranding Sargassum Samples. We performed principal component analysis (PCA) to visualize the elemental content of sargassum after different processing methods and across a full season of beaching. Cluster analysis supported the separation of the samples into two clusters, one corresponding to those harvested in May (F/frozen and S/shade-dried), June (F and S), July (F and S), and August (S) (cluster 1), and the other grouping samples collected in August (F), September (F and S), and October (F and S) (cluster 2) (*SI Appendix*, Fig. S1). No clear distinction was observed based on the method used for the processing of the samples, while discrimination was mainly supported by the month of sampling. Most of the variance (PC1 = 39.6%) was attributed to sampling before or after August, likely to be considered as a transition month during the year 2021. Separation along PC1 was related to differences in the content of K, As, and Na in the cluster 1 direction, and of Al, Ni, and Th in the cluster 2 direction. Within this latter cluster, the variance in PC2 direction (16.7%) supported the separation between samples harvested in September (F and S) and those collected in October (F and S) and August (F) and was mainly due to the differences in the content of Ba and Mn for the September direction, and of Ca, Mg, Tl in the August direction.

To complete this analysis, a more thorough assessment of the results was conducted. Only the main observations are reported here, and a more exhaustive description of these results, including p-values obtained by two-way ANOVA followed by the post hoc Holm–Sidak test, is given in *SI Appendix*, Text. Analysis of the elemental composition of sargassum showed significant differences

Table 2. Measured seawater and ash concentrations and estimated enrichment factors for seven selected elements determined in both ash and sargassum, and available in the eGEOTRACES atlas for samples collected along section GA02 (https://www.geotraces.org/geotraces-intermediate-data-product-2021/)

Elements	GEOTRACES concentration in the surface mixed layer (1)	Measured mean concentration in volcanic ash (ppm)	Estimated concentration in mixed layer after ash exposure (2)	Estimated seawater enrichment factor (2)/(1)
Al	~30 nmol kg^{-1}	87,652	760 μmol kg^{-1}.	~2.5×10^4
Fe	~0.5 nmol kg^{-1}	49,728	209 μmol kg^{-1}	~4.2×10^5
Mn	~2 nmol kg^{-1}	1,129	4.82 μmol kg^{-1}	~2,410
P	< 0.5 μmol kg^{-1}	515	3.90 μmol kg^{-1}	7.8 (minimum)
Zn	< 0.5 nmol kg^{-1}	79	0.283 μmol kg^{-1}	567 (minimum)
Co	~30 pmol kg^{-1}	17	0.142 μmol kg^{-1}	~4,700
Ni	~2 nmol kg^{-1}	13.5	0.054 μmol kg^{-1}	~27

in the total element content between frozen (170,069.34 ± 15,657.24 to 192,629.45 ± 1,608.91 ppm) and shade-dried (142,488.37 ± 1,003.70 to 187,196.53 ± 7,084.02 ppm) samples (Dataset S2 A–C). This was clear when comparing samples collected from July to October, in which the quantities of elements were constantly lower in shade-dried compared to frozen samples. When looking at monthly variations in total element content for each type of sample, the only significant difference for the frozen samples was observed between October and September. However, among the shade-dried samples, more statistically supported differences were found: Higher content of elements was quantified in July compared with May and June and lower amounts in September compared with all the other months except July.

A systematic examination of variations for individual elements quantified in sargassum samples was then conducted (Fig. 5). We only considered those for which content was determined to be higher than 1 ppm, so Se, Mo, Ag, Cd, Sb, TI, Pb, Th, U, and Co were excluded. The most abundant elements found in seaweed samples were K, Ca, Na, and Mg, with amounts above 10,000 ppm (Fig. 5*A*). Although significant variations were determined when comparing the influence of sample processing on the total content of elements, when looking at elements individually, limited statistical support was observed for the influence of processing methods, except for Na, Ca, and Ni. Based on this, and to improve clarity in subsequent analysis, only key statistically supported seasonal/monthly variations for the frozen samples will be described.

Similar variations were observed for K and Na, with higher amounts in May and June, lower in August, and then an increase in September and October (Fig. 5*A*). For Ca, the opposite trend was observed and content was higher in August compared to the other months. Among the elements for which a potential enrichment of seawater by volcanic ash was suggested, P, Fe, and Al were quantified in a similar range and showed a similar pattern of variations (Fig. 5*B*). Higher contents were detected in August, and, in most of the cases, remained high during September and October, with values above those measured in July and previous months. Similar results were observed for Mn (Fig. 5*C*). In contrast, As content decreased between July and August–September. Zn was not detected in sargassum harvested in May and June (Fig. 5*D*), but was quantified in samples collected in July and August, with further content increase in September–October. The content in Ni almost doubled between June and August, remaining above 5 ppm afterward. Similarly, higher levels of Cu and Ba were determined in September–October compared to May and June.

Biochemical Composition of Sargassum after Different Processing Methods and across a Full Season. PCA was used to evaluate the potential influence of processing methods and potential seasonal variations on biochemical parameters known to be important for the physiology of brown algae, as well as being relevant for the valorization of this biomass. Two distinct clusters were observed, one containing the frozen (F) samples, and the other corresponding to the shade-dried (S) samples (*SI Appendix*, Fig. S2). This suggests that most of the variance (PC1 = 31.5%) among the samples analyzed is due to the methods used to process the samples, in contrast with what was observed for the elemental composition of the same samples. The separation between the two clusters was due to differences between several parameters, including alginate_mono that corresponds to the percentage of the total sugars accounted for by alginate (mannuronic and guluronic acid), the content of fucoxanthin and phlorotannins in the direction of the F samples, and by the moisture content and the amounts of mannitol and glucose in the direction of the S samples. No clear trend was associated with the second component (PC2 = 28.6%), which was mainly supported by the differences in the protein and ash contents in one direction, and by differences in the amounts of several monosaccharides and uronic acids in the opposite direction.

Building on these results, a more in-depth investigation of the results was conducted, and the most relevant observations are reported in this section. A more exhaustive description, including p-values obtained by two-way ANOVA followed by the post hoc Holm–Sidak test, is presented in *SI Appendix*, Text. Ash produced from seaweed biomass represented 37 to 39% of the sargassum DW in frozen samples and 33 to 40% in samples after shade-drying (Fig. 6*A* and Dataset S3 A and B). Moisture accounted for 8 to 9% and 10 to 14% of biomass DW in frozen and shade-dried samples, respectively (Fig. 6*A* and Dataset S3 A and C). Very limited differences were observed across the period of sampling and between the sample processing methods for the ash and moisture contents in the samples investigated.

Protein content ranged between 28 and 36 mg/g biomass DW in frozen samples and 29 to 35 mg/g biomass DW in shade-dried samples (Fig. 6*B* and Dataset S4 A and B). No significant differences in the amount of proteins were determined between the two processing methods. A slight decrease in the amount of proteins was observed in June compared to other months. Quantities of phenolics were more variable and usually higher in the shade-dried (0.17 to 0.43 mg/g biomass DW) compared to the frozen samples (0.22 to 0.27 mg/g biomass DW) (Fig. 6*C* and Dataset S5 A and B). Very limited seasonality was detected for this class of compounds. Contents in phlorotannins were systematically lower in shade-dried (0.11 to 0.24 mg/g biomass DW) compared to frozen (0.22 to 0.32 mg/g biomass DW) samples (Fig. 6*C* and Dataset S5 A and C). Seasonal variations were observed only in the shade-dried samples,

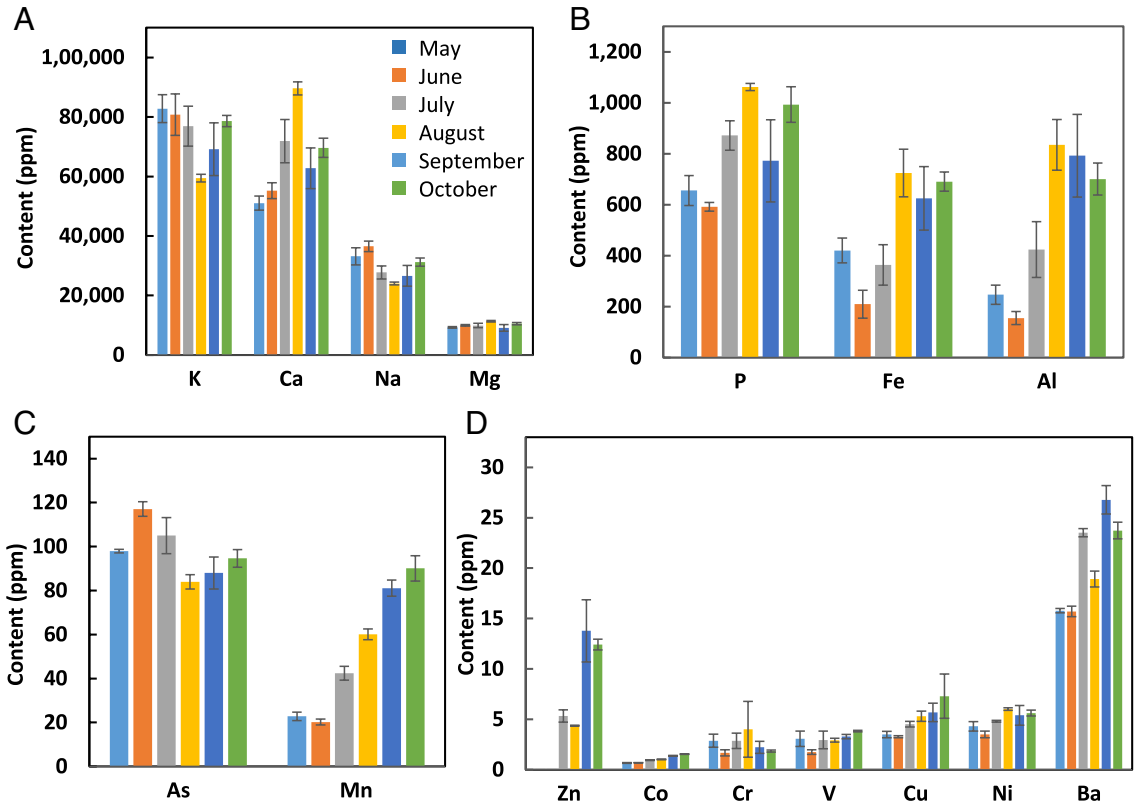

Fig. 5. Elemental composition of sargassum harvested in Jamaica across the 2021 sargassum inundation season. Samples were all frozen prior to analysis. For ease of visualization, elements were grouped by panel according to concentrations in seaweed biomass: (*A*) very high, (*B*) high, (*C*) medium, (*D*) low. The mean ± SD is reported for each measurement. Results of statistical analysis, including of the post hoc test, are provided in Dataset S2 A–C.

in particular a higher content in September and October compared to May, June, and July. The amounts of the pigment fucoxanthin were significantly higher in frozen samples (743 to 1,130 µg/g biomass DW) compared to shade-dried samples (33 to 54 µg/g biomass DW) (Fig. 6*D* and Dataset S6 A and B). There were also clear seasonal variations in the frozen samples with higher contents in August, September, and October compared to June and July, as suggested by PCA.

One of the trademarks of brown algae is the prevalence of peculiar complex polysaccharides and their monosaccharide composition. The total content of monosaccharides ranged between 142 to 183 and 113 to 205 mg/g biomass DW in frozen and shade-dried samples, respectively (Fig. 6*E* and Dataset S7 A–E). No clear trend was identified when assessing the impact of processing methods on the quantities of monosaccharides between frozen and shade-dried samples. In addition, no statistically supported seasonal variations were observed when comparing all the frozen samples. After shade-drying, only an increased amount of monosaccharides in September was observed when compared to all other months (except June).The most abundant monosaccharides were the mannuronic (M) and guluronic (G) acids, which are the subunits of the cell wall polysaccharide alginate. M content ranged between 69 and 89 mg/g and between 43 and 87 mg/g of biomass DW for the frozen and shade-dried samples respectively. For G, a wider range was observed in shade-dried (15 to 36 mg/g biomass DW) compared to frozen samples (31 to 37 mg/g biomass DW). No specific trend was identified between the processing methods for M, while higher amounts of G were quantified in frozen compared to shade-dried sample (except for September). No monthly differences in frozen samples were monitored for both M and G. Variations were observed in shade-dried with significant higher content of M and G in September compared to other months. Alginates accounted for 10 to 13% and 6 to 12% of the biomass DW in frozen and in shade-dried samples respectively, with usually significantly higher % in frozen compared to shade-dried samples. No statistically supported monthly variations were noticed in the frozen samples. In contrast, the shade-dried samples showed significant lower alginate % in May and July compared to June and September. The M:G ratios ranged between 2.17 and 2.41 for frozen samples, and 2.44 and 3.06 for shade-dried samples (*SI Appendix*, Fig. S3 and Dataset S7 B and E). Values were systematically higher in shade-dried compared to frozen samples, and no statistically supported monthly changes were observed within frozen or shade-dried samples.

Fucose is also an important monosaccharide in brown algae as a constituent (main chain or branching) of the fucose-containing sulfated polysaccharides that are a key component of the brown algal cell. It represented between 14 and 18 mg/g biomass DW in frozen samples, and 12 to 26 mg/g biomass DW in shade-dried samples. Content of this monosaccharide was generally higher in the latter, as statistically supported in June and September. Seasonal variations were observed only in shade-dried samples, in particular when comparing September with all other months (except June). The polyol (sugar alcohol) mannitol is a form of carbon storage produced from photosynthesis and is also involved in the physiological response triggered in brown algae under abiotic stress conditions. Higher quantities were measured in shade-dried (13 to 18 mg/g biomass DW) compared to frozen samples (2 to 14 mg/g biomass DW). Differences were statistically supported for the months July, September, and October. Seasonal variations were observed only in frozen samples, with statistical support for comparison between months with the lowest contents (July, September, October) and those with the higher amounts (May and June). Glucose is found in the cell wall polysaccharide cellulose and in the carbon storage

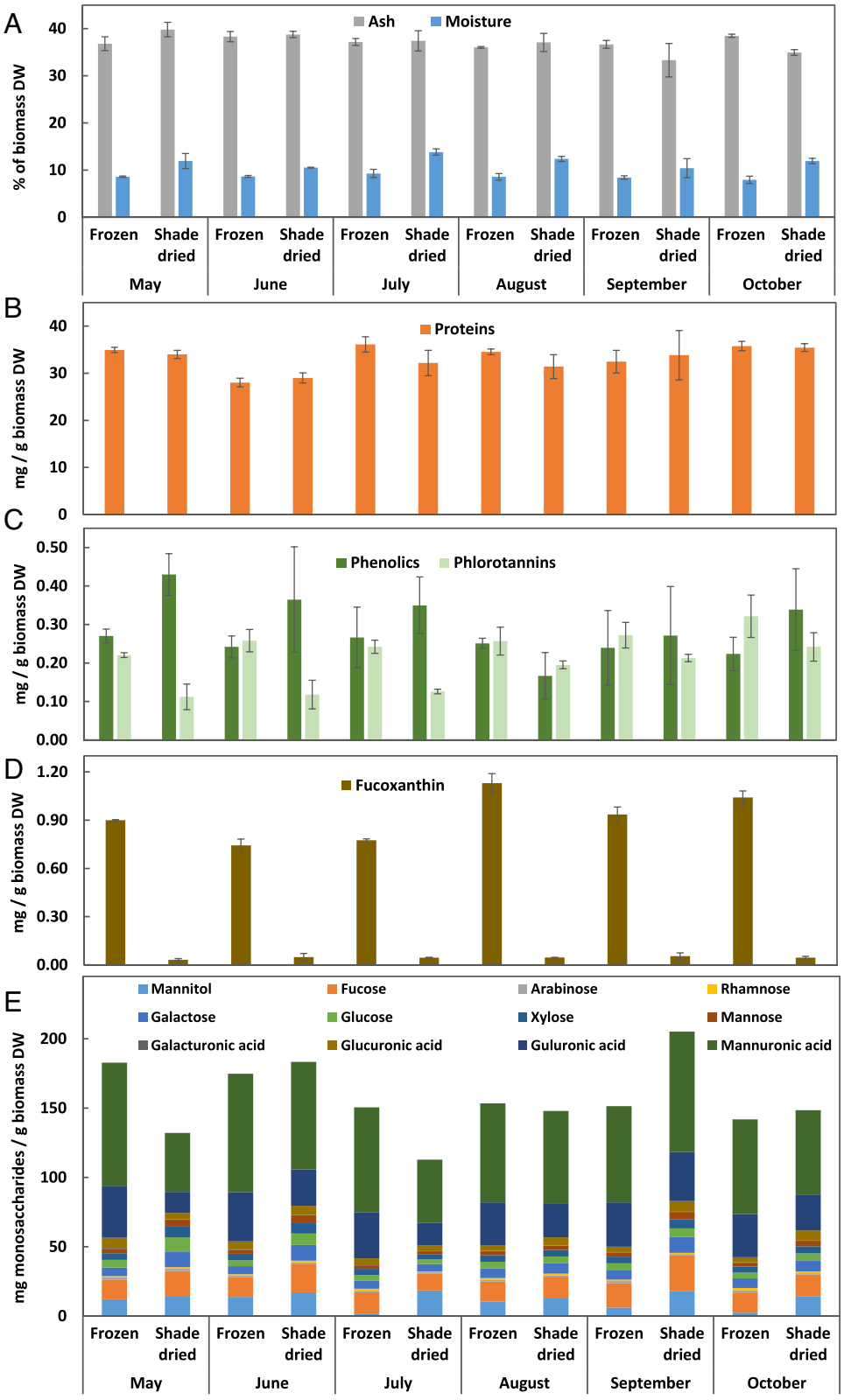

Fig. 6. Biochemical composition of sargassum harvested in Jamaica across the year 2021. Results show contents in ash and moisture (*A*), proteins (*B*), phenolics and phlorotannins (*C*), fucoxanthin (*D*), and monosaccharides (*E*). Results of statistical analysis, including of the post hoc test, are provided in Dataset S3 A–C for panel *A*, Dataset S4 A and B for panel *B*, Dataset S5 A–C for panel *C*, Dataset S6 A and B for panel *D*, and Dataset S7 A–E for panel *E*.

polysaccharide laminarin. It accounted for 4 to 6 mg/g biomass DW in frozen samples, and 3 to 10 mg/g biomass DW in shade-dried samples. Amounts of glucose were frequently higher in shade-dried samples, with significant differences for biomass harvested in May and June. No monthly differences were identified in the frozen samples. However, more glucose was found in shade-dried samples in May–June compared to July–August–September–October. Other less abundant monosaccharides and uronic acids (galactose, xylose, mannose, rhamnose, arabinose, glucuronic acid, and galacturonic acid) are discussed in *SI Appendix*, Text.

Potential Interactions between Biochemical and Elemental Composition. To explore possible interplay between the content of biochemical compounds and of elements, a correlation analysis was conducted using results obtained for the frozen/freeze-dried samples. Focusing on biochemical compounds, we found strong

correlations between mannuronic acid, guluronic acid, glucuronic acid, galacturonic acid, and mannose (*SI Appendix*, Fig. S4). Contents in fucose, xylose, mannose, glucose, and galactose were also significantly positively correlated. Negative correlations were observed between glucuronic acid and phlorotannins/fucoxanthin, as well as between proteins and mannitol. Regarding possible interactions between the elements, content of As was strongly negatively correlated with most of the elements investigated, including Al, P, Ca, V, Mn, Fe, Co, Ni, Zn, Ag, Pb, Th, and U, but positively correlated with Na and K content. Positive correlations were also observed between Mn, Fe, Co, Ni, Cu, Zn, Ba, Pb, Th, and U.

When assessing potential correlations between the content of elements and of biochemical compounds, the most interesting observations were probably the significant positive correlations between mannuronic acid, guluronic acid, glucuronic acid, and quantities of Na, K, and As, and the negative correlation between these uronic acids and most of the other elements (Fig. 7). Positive correlations between As and mannuronic and guluronic acids, the constituents of the cell wall polysaccharide alginate, is in line with results obtained in the other brown alga *Laminaria digitata* in which accumulation of As was found in the cell wall and the cell membranes (46). In addition, positive correlations were observed between fucoxanthin and Mg, Al, P, Ca, Mn, Fe, Co, Ni, Cu, Ag, TI, Th, and U, and negative correlations between this pigment and Na, K, and As. This observation suggests that fucoxanthin content may increase in response to some of these elements as part of antioxidative processes (47).

Discussion

During Caribbean sargassum influxes, *S. natans* I and VIII, and *S. fluitans* III have been shown to be the dominant morphotypes, and their relative abundance varied across seasons, years, and regions (31–35). *S. fluitans* III was the predominant morphotype on the Mexican Caribbean coast between September 2016 and May 2020 (31). In the same way, significant seasonal variation was observed in the relative abundance of the three morphotypes of sargassum in Barbados during the years 2021-2022 (34), and *S. fluitans* III was the main morphotype across the sampling period considered. Our results from Jamaica obtained for 2021 events showed a similar trend, with *S. fluitans* III being the most abundant morphotype observed after beaching, despite significant variations in relative abundance across the year. One explanation for this may be related to the higher growth rates observed for *S. fluitans* III at sea surface temperatures experienced within the Tropical Atlantic (i.e., >26 °C) when compared to the two *S. natans* morphotypes (48–50). It was further suggested that relative morphotype composition is likely linked to seasons, meteorological and oceanographic conditions, and to the oceanic suborigins of sargassum that may vary across the year (7, 34). In light of previous analysis showing some differences in the biochemical and elemental composition of individual morphotypes that may be of importance for valorization (43), we analyzed potential seasonal variations of stranded biomass composition, as well as influence of sample processing methods. For this, we focused on several classes of compounds important for the biology and uses of brown algae, and that we have already investigated in sargassum biomass, i.e., proteins, phenolics, phlorotannins, fucoxanthin, monosaccharides, and uronic acids (22, 51, 52).

No significant difference in the content of proteins was observed between frozen and shade-dried samples. Similar results were obtained when comparing sun-dried and frozen samples obtained for biomass harvested in the same location in Jamaica in summer 2020 (22), suggesting that processing methods do not significantly alter the amount of proteins in sargassum biomass. Although phenolic contents were frequently higher in shade-dried compared to frozen samples, results were difficult to interpret due to variations among some of the biological replicates. A lower content of phlorotannins in shade-dried samples was observed compared to frozen samples, and this is in contrast with previous results showing a higher content for these compounds in sun-dried compared to frozen samples (22). To explain this, we suggest that direct exposure to the sun may trigger higher phlorotannin biosynthesis than when shade-drying. For fucoxanthin, shade-drying showed similar impact as sun-drying as both processing methods greatly reduced the quantities of this pigment. While the total amount of monosaccharides was lower in sun-dried compared to frozen samples in 2020, no clear trend was observed in the current study, suggesting that shade-drying may be less detrimental for the total amount of monosaccharides than sun-drying. However, higher contents of alginate were usually quantified in frozen samples compared to shade-dried and sun-dried samples (22). Results obtained for both fucoxanthin and alginate therefore suggest that biomass should be processed shortly after harvesting to maximize extraction of these valuable compounds.

The eruption of the La Soufrière volcano in April 2021 provided the opportunity to investigate potential assimilation of elements contained in the ash by floating sargassum. It has already been reported that volcanic ash can fertilize iron-limited phytoplankton, in particular, diatoms which share some phylogenetic history with brown algae as both are Stramenopiles (38). Combined analysis of sargassum and volcanic ash drift suggests that ash and sargassum overlapped for about 50 d and that biomass arriving in Jamaica in early August was likely exposed to ash fallout. The overall limited monthly variations observed in the biochemical composition of sargassum harvested between May and October indicates that volcanic ash exposure had limited impact on the content of key compounds found in brown algal biomass. This is in contrast with observations made when focusing on elemental composition. We have calculated that volcanic ash had the potential to increase local seawater concentrations of P, Al, Fe, Mn, Zn, Co, and Ni. When examining the elemental composition of sargassum biomass beaching in Jamaica across the full 2021 year, with a focus on frozen samples, we observed significant increase in the content of P, Al, Fe, Mn, Zn, and Ni in algal samples harvested from August. We also noticed a significant decrease of As content in sargassum biomass beaching after July. Nevertheless, concentrations of this metalloid remained above maximum limits permitted for several potential applications of sargassum biomass including seaweed-derived meal and feed in Europe (40 µg/g DW) (53), and for agricultural soils in different countries (15 to 50 µg/g DW) (28). In plants, both phosphate and arsenic, owing to their structural similarity, are taken up through the same mechanisms (54). In line with this, and as observed in the samples analyzed in our study, a negative correlation between P and As content was observed in sargassum samples collected at sea (55) and after stranding (56). It has also been shown in diatoms that As toxicity and bioaccumulation decrease at elevated phosphate concentrations (57). This suggests that floating sargassum had taken up elements provided by the volcanic ash, and high concentrations were maintained during the advection of the mats from the Northern Tropical Atlantic to Jamaica. This elemental signature, apparent in sargassum after approximately 3 to 4 mo of travel from the volcanic fallout area to Jamaica, also supports that the sargassum biomass has remained alive and afloat and has not suffered significant mortality or sinking out of the surface layer over this time period. This is important information, given that little

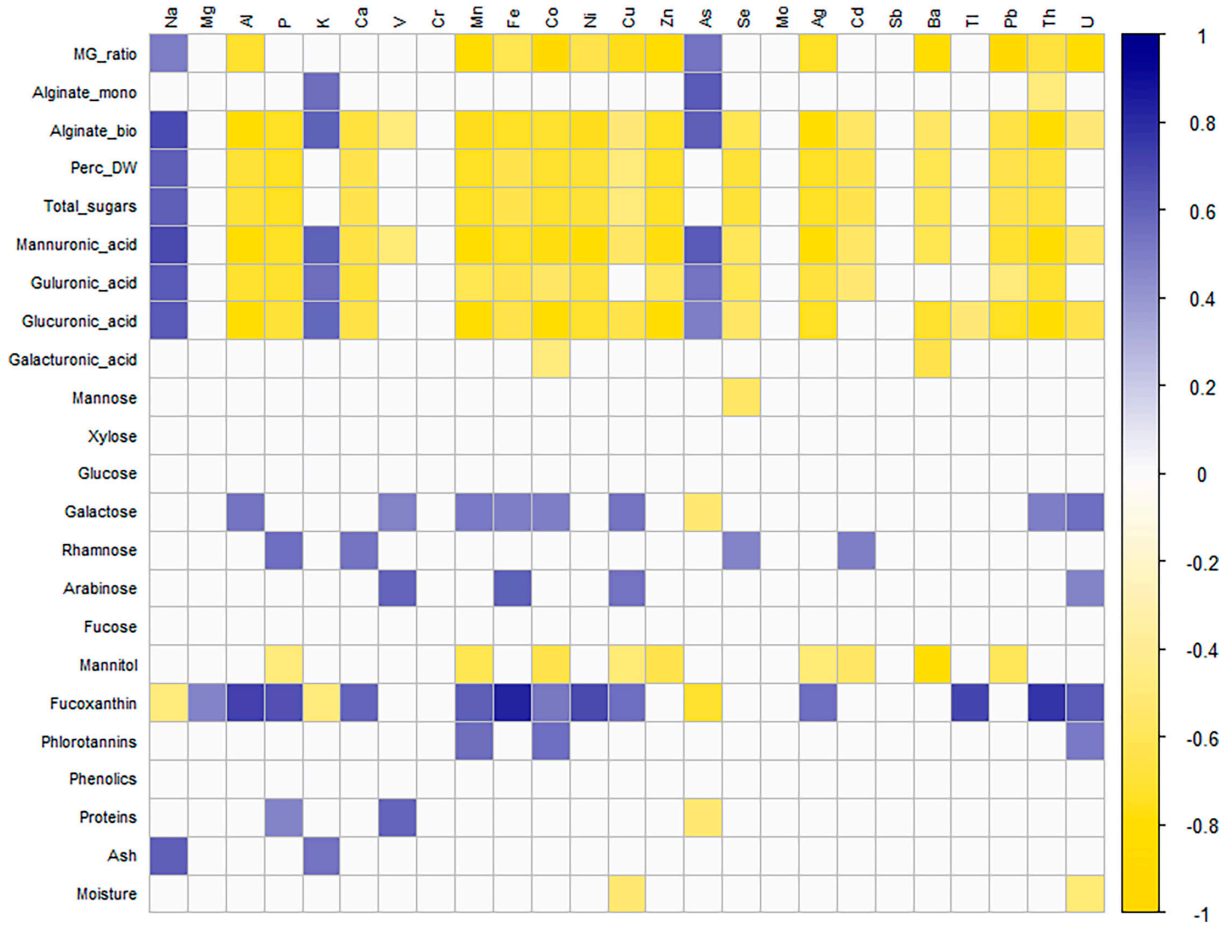

Fig. 7. Heat map showing potential correlations between the contents of biochemical compounds and of elements in freeze-dried sargassum biomass harvested at different times of the year 2021. Only significant correlations (*P*-value ≤ 0.05) are plotted. Alginate_bio, percentage of biomass accounted for by alginate (mannuronic and guluronic acids); Alginate_mono, percentage of the total sugars accounted for by alginate (mannuronic and guluronic acids); MG_ratio, mannuronic acid:guluronic acid (M:G) ratio; Perc_DW, percentage of the dry weight accounted for by the total quantities of sugars; Total sugars, total quantities of mannitol, monosaccharides, and uronic acids. An extended version of this figure is presented in *SI Appendix*, Fig. S4.

or nothing is known about the longevity of sargassum thalli, especially in the Tropical Atlantic.

Conclusion

In line with other recent studies in the Tropical Atlantic, *S. fluitans* III was consistently the dominant morphotype beaching in Jamaica from the Great Atlantic Sargassum Belt in 2021. Overall, the biochemical composition of sargassum in 2021 was quite homogenous throughout the year, showing no major seasonal variations, and no apparent impact from exposure to volcanic ash, except for the pigment fucoxanthin. This is important for valorization as consistency of feedstock is a key factor to consider for developing applications. In addition, changes in the biochemical composition observed between processing methods should be taken into consideration for the implementation of valorization pathways. Sargassum exposed to volcanic ash from La Soufrière volcano did show an increase in the elemental content of P, Al, Fe, Mn, Zn, Ni, and a decrease in As. However, As levels remained high enough to hamper some potential routes for uses of this biomass. In the future, it is important to continue monitoring over the long-term morphotype abundance, as well as biochemical and elemental biomass composition, not only for valorization, but also to assess the effect of atmosphere and ocean changes on the biology and ecology of sargassum.

Materials and Methods

Remote Sensing of Sargassum at the Regional Scale. To estimate the areal extent of sargassum in selected subregions, satellite images provided by the Optical Oceanography Laboratory at the University of South Florida via their website (https://optics.marine.usf.edu) were used. Daily maps of floating algae, "FA_density," were provided as the mean of the seven past days (including the current day) following a method previously described (58). FA_density images were assessed for three standardized regions: the Central Atlantic Region (38 to 63°W, 0 to 22°N); the Eastern Caribbean (60 to 75°W, 10 to 23°N); and around Jamaica (75 to 82°W, 15 to 22°N).

Simulation of Sargassum and of Volcanic Ash Drift. To trace the source of sargassum arriving near Jamaica, virtual "particles," which are subject to the winds and ocean currents of an eddy-resolving ocean model hindcast, were used. This hindcast dataset comprises 5-d averages of surface winds and currents over 1988 to 2010, obtained with the Nucleus for European Modelling of the Ocean (NEMO) ocean model (59) in eddy-resolving global configuration (ORCA12), henceforth NEMO-ORCA12. The ORCA12 configuration of NEMO has a horizontal resolution at the Equator of 1/12°, or 9.277 km, close to the resolution in previous sargassum drift calculations (60–62), and essential to best represent the swift and narrow boundary currents that dominate the region.

In forward tracking mode, particles are "released" hourly for 5 d in a triangular area representative of ash deposition to the east and south of St Vincent, with subsequent positions recorded at daily intervals for 90 d. The particle trajectories are calculated using the off-line Lagrangian ARIANE mass-preserving algorithm (63) in "qualitative mode," with the 5-d mean horizontal velocity fields of NEMO-ORCA12. ARIANE is based on an analytical solution for curvilinear particle

trajectories across model grid cells. In this study, particles are constrained to drift with surface currents and the trajectories are hence two-dimensional in the latitude–longitude plane. As in previous studies of sargassum drift (64–66), the surface-drifting particles representative of sargassum are also subject to "windage," here specified as 1%. Particles representative of ash are not subject to windage, which is hence specified as 0%.

Backtracking particles for up to 120 d from just east of Jamaica (prior to beaching, subject to 1% windage), we further assess the extent to which sargassum beaching in south Jamaica may be potentially influenced by ash from La Soufrière. Particle data from forward and backtracking experiments are statistically analyzed on a grid of resolution 0.5° × 0.5° for fractional presence (number of particle transitions through a grid cell divided by total number of transitions) and mean age (days adrift, since the experiment started). We run the backtracking experiment for 23 hindcast years spanning 1988 to 2010, to account for interannual variability in winds and currents.

Sampling of Sargassum and Determination of Morphotype Abundance. Sargassum was collected on six different occasions (May 1, June 5, July 12, August 12, September 13, and October 13, 2021) from Fort Rocky Beach, Port Royal, Jamaica (17°56′13.9″N 76°49′02.8″W). The algal biomass was obtained by wading into the surf (in less than 1 m of water) and using a "surf net" to collect ~7 kg portions from the water column. After transport to the laboratory and cleaning of non-sargassum debris, three 2 kg portions of the freshly cleaned biomass had the three dominant morphotypes (*S. natans I*, *S. natans VIII*, and *S. fluitans III*) separated visually, so morphotype ratios could be determined. The separated portions were spread to dry in the shade where daytime temperatures ranged from 28.2 to 32.5 °C and night-time temperatures from 25.0 to 27.2 °C. The material was allowed to shade-dry for 36 h after which each subsample's morphotypes were weighed, recombined, and packaged for shipment. In addition, three 100 g portions of the unseparated biomass were packaged in separate Ziploc® bags, frozen using liquid nitrogen within 2 h of packaging, and stored at −20 °C. All fresh sample processing was completed within 3 h of collecting from the sea. Frozen samples were then freeze-dried for 48 h in a Heto Power Dry PL3000 freeze dryer (Thermo Fisher Scientific). Both frozen and sun-dried samples were milled to 1 mm diameter particle size using a SM 300 cutting mill (Retsh), and stored before subsequent analysis.

Sampling of Volcanic Ash. Two samples of ash that had fallen on Barbados from 11 to 13 April 2021 during the main deposition event were analyzed. Sample 1 was collected on the 11th of April 2022, and sample 2 on the 13th of April 2022 in Barbados, GPS coordinates 13°09′13.6″N 59°36′52.0″W.

Elemental Analysis of Seaweed and Volcanic Ash Samples. Approximately 0.1 g of dried sargassum samples was digested using a CEM MARS 6 microwave digest system in 5 mL of concentrated subboiled nitric acid at 200 °C for 15 min and then diluted with Milli-Q water before being subsampled and further diluted to give an overall dilution of approximately 2,100 for further inductively coupled plasma mass spectrometry analysis. The resulting samples were spiked to give an In and Re final concentration of 5 ppb to act as internal standards. The standards were made from the IV-Stock-50 Inorganic Ventures environmental Standard and were also spiked with In and Re at 5 ppb final concentrations. A suite of P standards were also made from Inorganic Ventures single element P standard.

For the ash, approximately 0.1 g of the sample was weighed into a 15 mL Savillex Teflon vial and digested in a mixture of subboiled concentrated nitric acid and concentrated hydrofluoric acid (Romil SpA grade) sealed on a hotplate at 130 °C overnight. The digestion acid was dried off and the samples redissolved in 6 M HCl before being dried and redissolved to make a mother solution in ~3M HCl. A subsample was taken, dried, and redissolved in 3% nitric acid, containing 5 ppb In and Re and 20 ppb Be to act as internal standards, to give a total dilution of ~4,000. They were then analyzed against a suite of international rock standards (Jb-2, JB-3, JGb-1, BHVO2, AGV-2, BCR-2, BIR-1, JG-2, and JR-2) and the same standards as mentioned above to obtain the As concentration. All seaweed and ash samples were run on an Agilent 8900 TripleQuad inductively coupled plasma mass spectrometer (QQQ-ICP-MS) using standard He, He-HMI, and oxygen modes depending on the element of interest.

Biochemical Analysis of Seaweed Samples. Contents of ash, moisture, proteins, phenolics, phlorotannins, fucoxanthin, monosaccharides, and alginates were determined as previously described (22).

Statistical Analyses. Statistical tests for investigating potential significance of changes in the abundance of the morphotypes across the six months of sampling were conducted using SPSS Version 22. Shapiro–Wilk analysis was used to test normality among all the parameters, and due to the assumptions of the data, a univariate two-way ANOVA was performed, followed by a post hoc Tukey test for all pairwise comparisons. The level of significance was set at P-value ≤0.05.

Potential variations in the biochemical and elemental composition of the biomass related to months of collection and processing of samples (frozen and shade-dried) were investigated following several approaches. PCA and cluster analysis were performed in RStudio on UV (unit variance)-scaled data to give all variables equal influence on the analyses. Data were further analyzed using SigmaPlot version 14.5. They were tested for normality using the Shapiro–Wilk test and homogeneity of variance by the Brown–Forsythe test. Then, two-way ANOVA was performed, followed by a post hoc Holm–Sidak test for all pairwise multiple comparisons. The significance level was fixed at P-value ≤0.05 for all the data analyses.

To explore possible relationships between biochemical and elemental composition, a test of association between paired samples using Pearson's product moment correlation coefficient was performed using RStudio. The level of significance was set at P-value ≤0.05.

Data, Materials, and Software Availability. The satellite datasets analyzed for this study can be found at the website of the Optical Oceanography Laboratory at the University of South Florida (https://optics.marine.usf.edu) (58), selecting "Satellite Data Products," and further selecting: "E. Caribbean" and "Jamaica" from "Caribbean"; "Central Atlantic" from "South America." To download all daily FA_density images for the E. Caribbean, Jamaica and Central Atlantic regions, we used Matlab scripts that are archived on Zenodo (DOI: 10.5281/zenodo.4899192) (67). Particle statistics (forward tracking) and primary particle data (backward tracking), along with the software used for the statistical analysis in Figs. 2 and 3, are also archived on Zenodo (DOI: 10.5281/zenodo.11086132) (68). Seawater concentrations of elements used for calculation in Table 2 are available at https://www.geotraces.org/geotraces-intermediate-data-product-2021/ (43). The ORCA12 hindcast dataset (archived at National Oceanography Centre, Southampton, UK) has been partly lost through disk failure, subsequent to use in the drift calculations.

ACKNOWLEDGMENTS. This publication is supported by the United Kingdom Economic and Social Research Council through the Global Challenges Research Fund (GCRF) project "Teleconnected SARgassum risks across the Atlantic: building capacity for TRansformational Adaptation in the Caribbean and West Africa (SARTRAC)," grant number ES/T002964/1. Further support is provided by the UK Natural Environment Research Council through the Urgency Grant project "Monitoring a large Sargassum bloom subject to a major volcanic eruption (MONISARG)", grant number NE/W004798/1. We also acknowledge support from the Caribbean Biodiversity Fund project, Adapting to a new reality: managing responses to influxes of sargassum seaweed in the Eastern Caribbean (SargAdapt), cofinanced by the International Climate Initiative of the German Federal Ministry for Environment, Nature Conservation, and Nuclear Safety through KfW. The ICP-MS analysis of elemental composition was undertaken by Matt Cooper, in the Geochemistry Research Group of the School of Ocean and Earth Science at the University of Southampton. We thank Dr. Michael Ross for sharing insights on protein determination in seaweed samples, Dr. Nicola Oates, Rachael Simister, and Dr. Leonardo Gomez for their help with the fucoxanthin analysis and for their assistance with the determination of monosaccharide contents, and Prof Julie Wilson for her insight on the use of statistical methods. Finally, we also thank the anonymous reviewers for their comments and suggestions that helped improve the final manuscript.

Author affiliations: [a]Centre for Novel Agricultural Products, Department of Biology, University of York, York YO10 5DD, United Kingdom; [b]School of Ocean and Earth Science, University of Southampton, Southampton SO14 3ZH, United Kingdom; [c]Department of Mathematics, University of York, York YO10 5DD, United Kingdom; [d]Centre for Resource Management and Environmental Studies, University of the West Indies, Cave Hill BB 11000, Barbados; [e]Centre for Marine Sciences, Department of Life Sciences, University of the West Indies, Mona Kingston 7, Jamaica; and [f]Department of Life Sciences, University of the West Indies, Mona Kingston 7, Jamaica

1. R. Bermejo, L. Green-Gavrielidis, G. Gao, Macroalgal blooms in a global change context. *Front. Mar. Sci.* **10**, 1204117 (2023).
2. United Nations Environment Programme-Caribbean Environment Programme, "Sargassum White Paper – Turning the crisis into an opportunity. Ninth Meeting of the Scientific and Technical Advisory Committee (STAC) to the Protocol Concerning Specially Protected Areas and Wildlife (SPAW) in the Wider Caribbean Region" (2021). https://www.unep.org/cep/resources/publication/sargassum-white-paper-turning-crisis-opportunity. Accessed 8 May 2023.
3. M. Wang *et al.*, The great Atlantic Sargassum belt. *Science* **365**, 83–87 (2019).
4. Y. A. Fidai, J. Dash, E. L. Tompkins, T. Tonon, A systematic review of floating and beach landing records of Sargassum beyond the Sargasso Sea. *Environ. Res. Commun.* **2**, 122001 (2020).
5. N. Skliris, M. Marsh, K. A. Addo, H. A. Oxenford, Physical drivers of pelagic sargassum bloom inter-annual variability in the Central West Atlantic over 2010–2020. *Ocean Dyn.* **72**, 383–404 (2022).
6. B. E. Lapointe *et al.*, Nutrient content and stoichiometry of pelagic *sargassum* reflects increasing nitrogen availability in the Atlantic Basin. *Nat. Commun.* **12**, 3060 (2021).
7. R. Marsh *et al.*, Climate-*sargassum* interactions across scales in the tropical Atlantic. *PLoS Clim.* **2**, e0000253 (2023).
8. A. E. Parr, Quantitative observations on the pelagic *sargassum* vegetation of the Western North Atlantic. *Bull. Bingham Oceanogr. Coll.* **6**, 1–94 (1939).
9. J. M. Schell, D. S. Goodwin, A. N. S. Siuda, Recent *sargassum* inundation events in the Caribbean: Shipboard observations reveal dominance of a previously rare form. *Oceanography* **28**, 8–10 (2015).
10. C. Hu, M. Wang, B. E. Lapointe, R. A. Brewton, F. J. Hernandez, On the Atlantic pelagic Sargassum's role in carbon fixation and sequestration. *Sci. Total Environ.* **781**, 146801 (2021).
11. A. Desrochers, S.-A. Cox, H. A. Oxenford, B. van Tussenbroek, "Sargassum Uses Guide: A Resource for Caribbean Researchers, Entrepreneurs and Policy Makers" (Tech. Rep. 97, University of the West Indies, Bridgetown, Barbados, 2020).
12. E. Aparicio *et al.*, High-pressure technology for *Sargassum* spp biomass pretreatment and fractionation in the third generation of bioethanol production. *Biores. Technol.* **329**, 124935 (2021).
13. U.C. Marx, J. Roles, B. Hankamer, *Sargassum* blooms in the Atlantic Ocean–From a burden to an asset. *Algal Res.* **54**, 102188 (2021).
14. T. M. Thompson, B. R. Young, S. Baroutian, Pelagic *Sargassum* for energy and fertiliser production in the Caribbean: A case study on Barbados. *Renew. Sust. Energ. Rev.* **118**, 109564 (2020).
15. T. M. Thompson, B. R. Young, S. Baroutian, Enhancing biogas production from Caribbean pelagic *Sargassum* utilising hydrothermal pretreatment and anaerobic co-digestion with food waste. *Chemosphere* **275**, 130035 (2021).
16. H. A. López-Aguilar *et al.*, Practical and theoretical modeling of anaerobic digestion of *Sargassum* spp. in the Mexican Caribbean. *Pol. J. Environ. Stud.* **30**, 3151–3161 (2021).
17. S. Saldarriaga-Hernandez, G. Hernandez-Vargas, H. M. N. Iqbal, D. Barceló, R. Parra-Saldívar, Bioremediation potential of *Sargassum* sp. Biomass to tackle pollution in coastal ecosystems: Circular economy approach. *Sci. Total Environ.* **715**, 136978 (2020).
18. C. Trench *et al.*, Application of stranded pelagic *sargassum* biomass as compost for seedling production in the context of mangrove restoration. *Front. Environ. Sci.* **10**, 932293 (2022).
19. A. A. Abdool-Ghany *et al.*, Assessing quality and beneficial uses of *Sargassum* compost. *Waste Manage.* **171**, 545–556 (2023).
20. V. Dominguez Almela *et al.*, Science and policy lessons learned from a decade of adaptation to the emergent risk of *sargassum* proliferation across the tropical Atlantic. *Environ. Res. Commun.* **5**, 061002 (2023), 10.1088/2515-7620/acd493.
21. S. van der Plank *et al.*, Polycentric governance, coordination and capacity: The case of *Sargassum* influxes in the Caribbean. *Coast. Manage.* **50**, 205–285 (2022).
22. C. B. Machado *et al.*, Pelagic *Sargassum* events in Jamaica: Provenance, morphotype abundance, and influence of sample processing on biochemical composition of the biomass. *Sci. Total Environ.* **817**, 152761 (2022).
23. H. A. Oxenford, S.-A. Cox, B. I. van Tussenbroek, A. Desrochers, Challenges of turning the sargassum crisis into gold: Current constraints and implications for the Caribbean. *Phycology* **1**, 27–48 (2021).
24. European Commission, Executive Agency for Small and Medium-sized Enterprises, Sijtsma, L., Guznajeva, T., Le Gallou, M., et al., Blue Bioeconomy Forum: Roadmap for the blue bioeconomy, Publications Office (2020), https://data.europa.eu/doi/10.2826/605949. Last Access 11 July 2023.
25. B. V. Nielsen *et al.*, Chemical characterisation of *Sargassum* inundation from the Turks and Caicos: Seasonal and post stranding changes. *Phycology* **1**, 143–162 (2021).
26. S. Saldarriaga-Hernandez, E. M. Melchor-Martínez, D. Carrillo-Nieves, R. Parra-Saldívar, H. M. N. Iqbal, Seasonal characterization and quantification of biomolecules from *Sargassum* collected from Mexican Caribbean coast–A preliminary study as a step forward to blue economy. *J. Environ. Manag.* **298**, 113507 (2021).
27. P. A. Ortega-Flores *et al.*, Trace elements in pelagic *Sargassum* species in the Mexican Caribbean: Identification of key variables affecting arsenic accumulation in *S. fluitans*. *Sci. Total Environ.* **806**, 150657 (2022).
28. R. E. Rodríguez-Martínez *et al.*, Element concentrations in pelagic *sargassum* along the Mexican Caribbean coast in 2018–2019. *PeerJ* **8**, e8667 (2020).
29. K. Alleyne, F. Neat, H. A. Oxenford, An analysis of arsenic concentrations associated with *sargassum* influx events in Barbados. *Mar. Pollut. Bull.* **192**, 115064 (2023).
30. P. A. Ortega-Flores *et al.*, Inorganic arsenic in holopelagic *Sargassum* spp. stranded in the Mexican Caribbean: Seasonal variations and comparison with international regulations and guidelines. *Aquat. Bot.* **188**, 103674 (2023).
31. M. García-Sánchez *et al.*, Temporal changes in the composition and biomass of beached pelagic *Sargassum* species in the Mexican Caribbean. *Aquat. Bot.* **167**, 103275 (2020).
32. R. Cabrera *et al.*, Registro de arribazón inusual de *Sargassum* (Phaeophyceae) para la costa Atlántica de Costa Rica. *Hidrobiológica* **31**, 31–42 (2021).
33. L. A. Iporac *et al.*, Community-based monitoring reveals spatiotemporal variation of Sargasso inundation levels and morphotype dominance across the Caribbean and South Florida. *Aquat. Bot.* **182**, 103546 (2022).
34. K. S. T. Alleyne, D. Johnson, F. Neat, H. A. Oxenford, H. Vallès, Seasonal variation in morphotype composition of pelagic *Sargassum* influx events is linked to oceanic origin. *Sci Rep.* **13**, 3753 (2023).
35. E. G. Torres-Conde, B. I. van Tussenbroek, R. E. Rodríguez-Martínez, B. Martínez-Daranas, Temporal changes in the composition of beached Holopelagic *Sargassum* spp. along the Northwestern Coast of Cuba. *Phycology* **3**, 405–412 (2023).
36. A. P. Poulidis *et al.*, Meteorological controls on local and regional volcanic ash dispersal. *Sci. Rep.* **8**, 6873 (2018).
37. I. A. Taylor *et al.*, A satellite chronology of plumes from the April 2021 eruption of La Soufrière, St Vincent. *Atmos. Chem. Phys.* **23**, 15209–15234 (2023).
38. B. Langmann, K. Zakšek, M. Hort, S. Duggen, Volcanic ash as fertiliser for the surface ocean. *Atmos. Chem. Phys.* **10**, 3891–3899 (2010).
39. E. P. Achterberg *et al.*, Natural iron fertilization by the Eyjafjallajökull volcanic eruption. *Geophys. Res. Lett.* **40**, 921–926 (2013).
40. R. Marsh *et al.*, Seasonal predictions of holopelagic *Sargassum* across the Tropical Atlantic accounting for uncertainty in drivers and processes: The SARTRAC Ensemble Forecast System. *Front. Mar. Sci.* **8**, 722524 (2021).
41. A. Anton *et al.*, Iron deficiency in seagrasses and macroalgae in the Red Sea is unrelated to latitude and physiological performance. *Front. Mar. Sci.* **5**, 74 (2018).
42. B. E. Lapointe, Phosphorus-limited photosynthesis and growth of *Sargassum natans* and *Sargassum fluitans*(Phaeophyceae) in the western North Atlantic. *Deep-Sea Res. Part A* **33**, 391–399 (1986).
43. R. Middag *et al.*, Dissolved aluminium in the ocean conveyor of the West Atlantic Ocean: Effects of the biological cycle, scavenging, sediment resuspension and hydrography. *Mar. Chem.* **177**, 69–86 (2015).
44. T. P. Boyer *et al.*, World Ocean Atlas 2018. [surface phosphate] (NOAA National Centers for Environmental Information, 2018). Dataset Accessed 4 April 2022.
45. C. de Boyer Montégut, G. Madec, A. S. Fischer, A. Lazar, D. Iudicone, Mixed layer depth over the global ocean: An examination of profile data and a profile-based climatology. *J. Geophys. Res.* **109**, C12003 (2004).
46. E. Ender *et al.*, Why is NanoSIMS elemental imaging of arsenic in seaweed (*Laminaria digitata*) important for understanding of arsenic biochemistry in addition to speciation information? *J. Anal. At. Spectrom.* **34**, 2291–2302 (2019).
47. G. B. Costa *et al.*, Physiological damages of *Sargassum cymosum* and *Hypnea pseudomusciformis* exposed to trace metals from mining tailing. *Environ. Sci. Pollut. Res.* **26**, 36486–36498 (2019).
48. M. Corbin, H. A. Oxenford, Assessing growth of pelagic *sargassum* in the Tropical Atlantic. *Aquat. Bot.* **187**, 103654 (2023).
49. E. Magaña-Gallegos *et al.*, Growth rates of pelagic *Sargassum* species in the Mexican Caribbean. *Aquat. Bot.* **185**, 103614 (2023a).
50. E. Magaña-Gallegos *et al.*, The effect of temperature on the growth of holopelagic *Sargassum* species. *Phycology* **3**, 138–146 (2023b).
51. D. Davis *et al.*, Biomass composition of the golden tide pelagic seaweeds *Sargassum fluitans* and *S. natans* (morphotypes I and VIII) to inform valorisation pathways. *Sci. Total Environ.* **762**, 143134 (2021).
52. T. Tonon *et al.*, Biochemical and elemental composition of pelagic *sargassum* biomass harvested across the Caribbean. *Phycology* **2**, 204–215 (2022).
53. Official Journal of the European Union, Commission regulation (EU) 2019/1869 of 7 November 2019 amending and correcting annex I to directive 2002/32/EC of the European Parliament and of the council as regards maximumlevels for certain undesirable substances in animal feed (2019). https://eur-lex.europa.eu/legal-content/EN/TXT/PDF/?uri=CELEX:32019R1869&from=EN. Accessed 11 July 2023.
54. N. Kandhol, V. P. Singh, L. Herrera-Estrella, L. P. Tran, D. K. Tripathi, Arsenite: The umpire of arsenate perception and responses in plants. *Trends Plant. Sci.* **27**, 420–422 (2022).
55. D. J. McGillicuddy *et al.*, Nutrient and arsenic biogeochemistry of *Sargassum* in the western Atlantic. *Nat. Commun.* **14**, 6205 (2023).
56. T. Gobert *et al.*, Trace metal content from holopelagic *Sargassum* spp. sampled in the tropical North Atlantic Ocean: Emphasis on spatial variation of arsenic and phosphorus. *Chemosphere* **308**, 136186 (2022).
57. Q. Ma, L. Chen, L. Zhang, Effects of phosphate on the toxicity and bioaccumulation of arsenate in marine diatom *Skeletonema costatum*. *Sci. Total Environ.* **857**, 159566 (2023).
58. M. Q. Wang, C. M. Hu, Mapping and quantifying *Sargassum* distribution and coverage in the Central West Atlantic using MODIS observations. *Remote Sens. Environ.* **183**, 356–367 (2016).
59. G. Madec, NEMO reference manual, ocean dynamic component: NEMO-OPA. Rep. 27, Note du pôle de modélisation, Institut Pierre Simmon Laplace (IPSL), France, ISSN No. 1288–1619 (2015).
60. N. F. Putman *et al.*, Simulating transport pathways of pelagic *Sargassum* from the Equatorial Atlantic into the Caribbean Sea. *Prog. Oceanogr.* **165**, 205–214 (2018).
61. M. T. Brooks, V. J. Coles, R. R. Hood, J. F. R. Gower, Factors controlling the seasonal distribution of pelagic *Sargassum*. *Mar. Ecol. Prog. Ser.* **599**, 1–18 (2018).
62. E. M. Johns *et al.*, The establishment of a pelagic *Sargassum* population in the Tropical Atlantic: Biological consequences of a basin-scale long distance dispersal event. *Prog. Oceanogr.* **182**, 102269 (2020).
63. B. Blanke, S. Raynaud, Kinematics of the Pacific Equatorial Undercurrent: An Eulerian and Lagrangian approach from GCM results. *J. Phys. Oceanogr.* **27**, 1038–1053 (1997).
64. D. R. Johnson, J. S. Franks, H. A. Oxenford, S. L. Cox, Pelagic *sargassum* prediction and marine connectivity in the tropical Atlantic. *Gulf. Caribbean Res.* **31**, GCFI20-GCFI30 (2020).10.18785/gcr.3101.15
65. N. F. Putman, R. Lumpkin, M. J. Olascoaga, J. Trinanes, G. J. Goni, Improving transport predictions of pelagic *Sargassum*. *J. Exper. Mar. Biol. Ecol.* **529**, 151398 (2020).
66. L. Berline *et al.*, Hindcasting the 2017 dispersal of *Sargassum* algae in the Tropical North Atlantic. *Mar. Pollut. Bull.* **158**, 111431 (2020).
67. R. Marsh, Seasonal predictions of holopelagic sargassum across the tropical Atlantic accounting for uncertainty in drivers and processes: the SARTRAC Ensemble Forecast System - scripts for downloading AFAI satellite data. Zenodo. https://doi.org/10.5281/zenodo.4899193. Deposited 4 June 2021.
68. R. Marsh, Changes in holopelagic Sargassum spp. biomass composition across an unusual year - supporting particle data and analysis source code [Data set]. Zenodo. https://doi.org/10.5281/zenodo.11086133. Deposited 29 April 2024.